Multi-omic analysis supports a developmental hierarchy of molecular subtypes in HGS ovarian carcinoma

Ludwig Geistlinger, Seyhun Oh, Marcel Ramos, Lucas Schiffer,
Boris Winterhoff, Martin Morgan, Giovanni Parmigiani, Michael Birrer,
Li-Xuan Qin, Markus Riester, Tim Starr, Levi Waldron

Supplementary Material

Contents

List of Figures

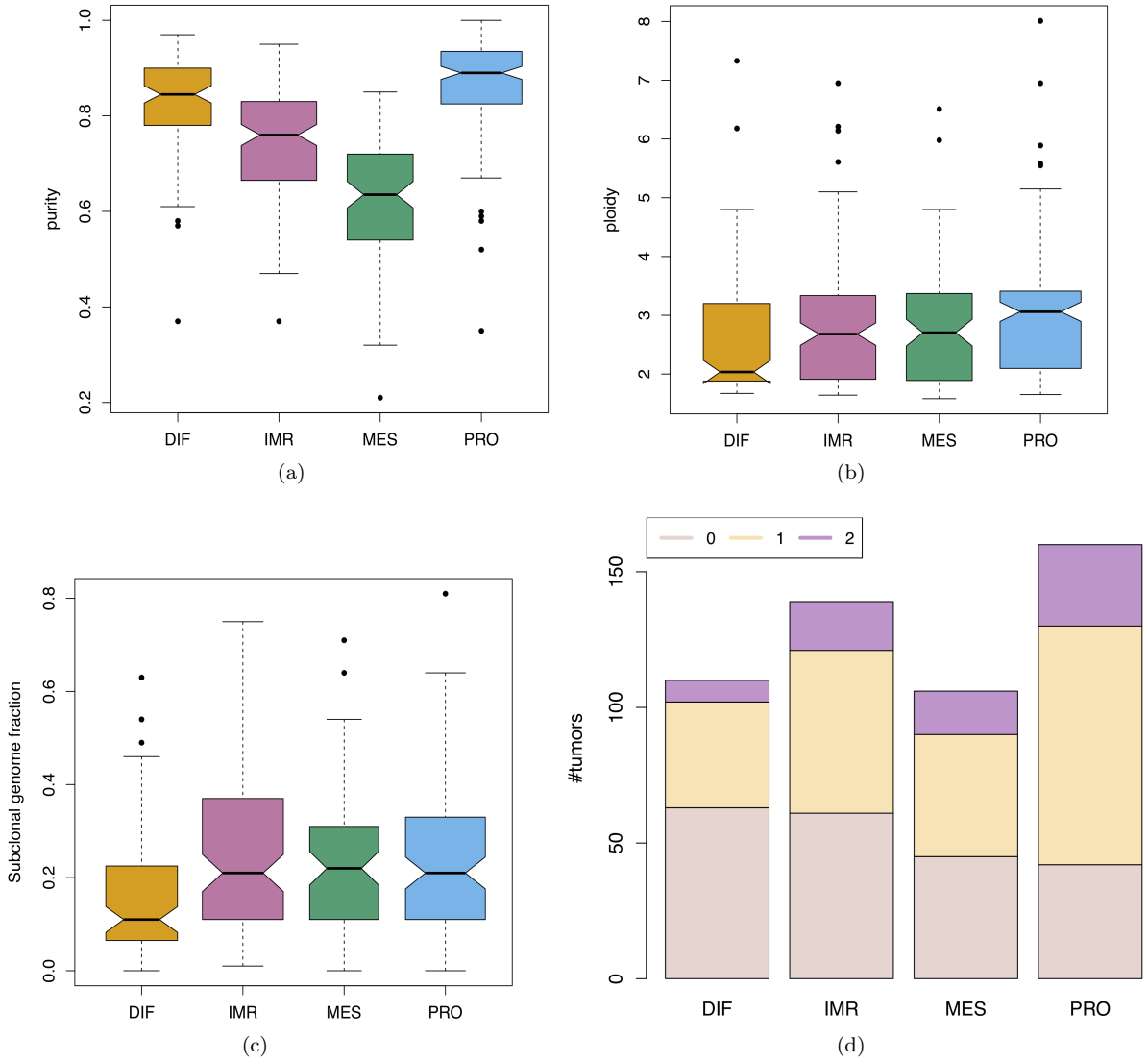

Figure S1: Tumors of differentiated subtype are characterized by high purity, but significantly lower ploidy, subclonality, and number of genome doublings than the other three subtypes. Subtype-stratified **(a)** purity, **(b)** ploidy, **(c)** subclonal genome fraction, and **(d)** number of genome doublings (0, 1, or 2) of TCGA HGS ovarian tumors as inferred by `ABSOLUTE`. Statistical significant differences in purity ($p < 2^{-16}$), ploidy ($p = 0.0026$), and subclonal genome fraction ($p = 0.0041$) were observed between subtypes using one-way ANOVA. The number of genome doublings also differed significantly between subtypes ($p = 8.2^{-5}$, χ^2 test, $df = 6$).

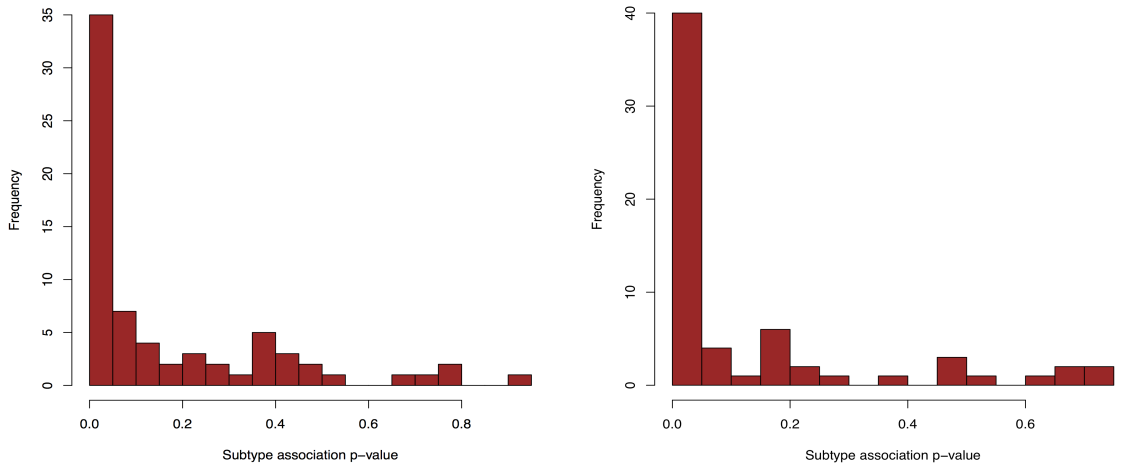

(a) OV (b) SARC

Figure S2: Association of SCNAs with transcriptome clusters. Shown is the distribution of nominal p-values as resulting from testing (χ^2 test with $df = 6$) recurrent focal SCNAs detected with `GISTIC2` for association with the TCGA transcriptome clusters for **(a)** 516 HGS ovarian tumors (70 SCNAs), and **(b)** 259 soft tissue sarcomas (64 SCNAs). See also Figure 3 of the main manuscript.

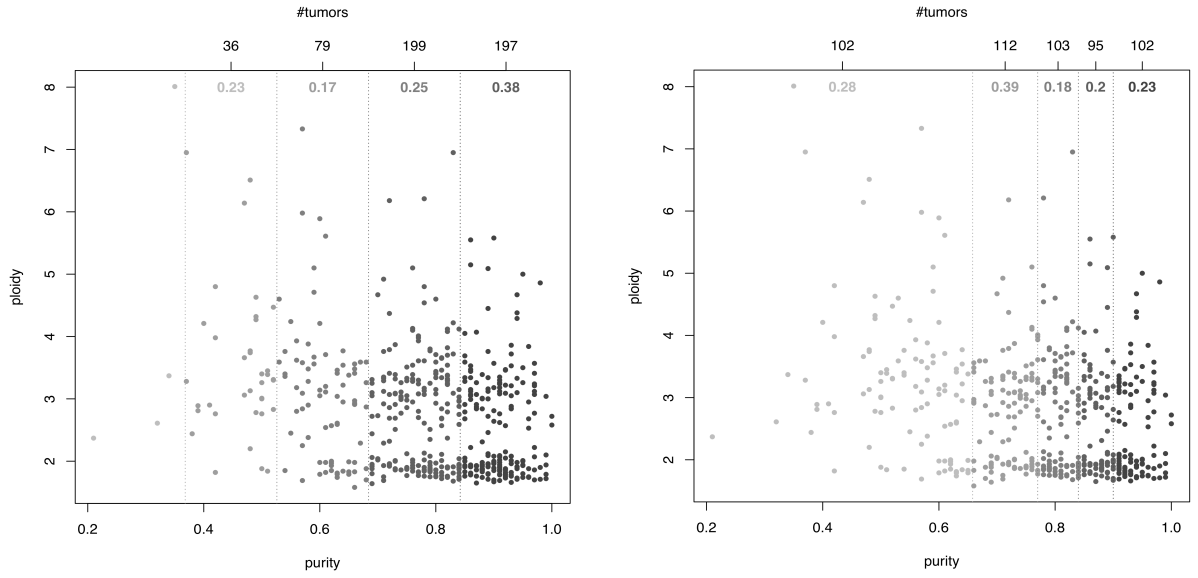

(a) equal bins (b) quintiles

Figure S3: Purity-stratified analysis. The scatterplots show purity (x-axis) and ploidy (y-axis) of 516 HGS ovarian tumors as stratified by purity in **(a)** equal bins, and **(b)** quintiles. The number of tumors in each stratum is indicated on top of each plot. The correlation of subtype association and subclonality $\rho(S_A, S_C)$ is shown at the top of each stratum, except for the first stratum in **(a)** due to insufficient sample size (4 tumors).

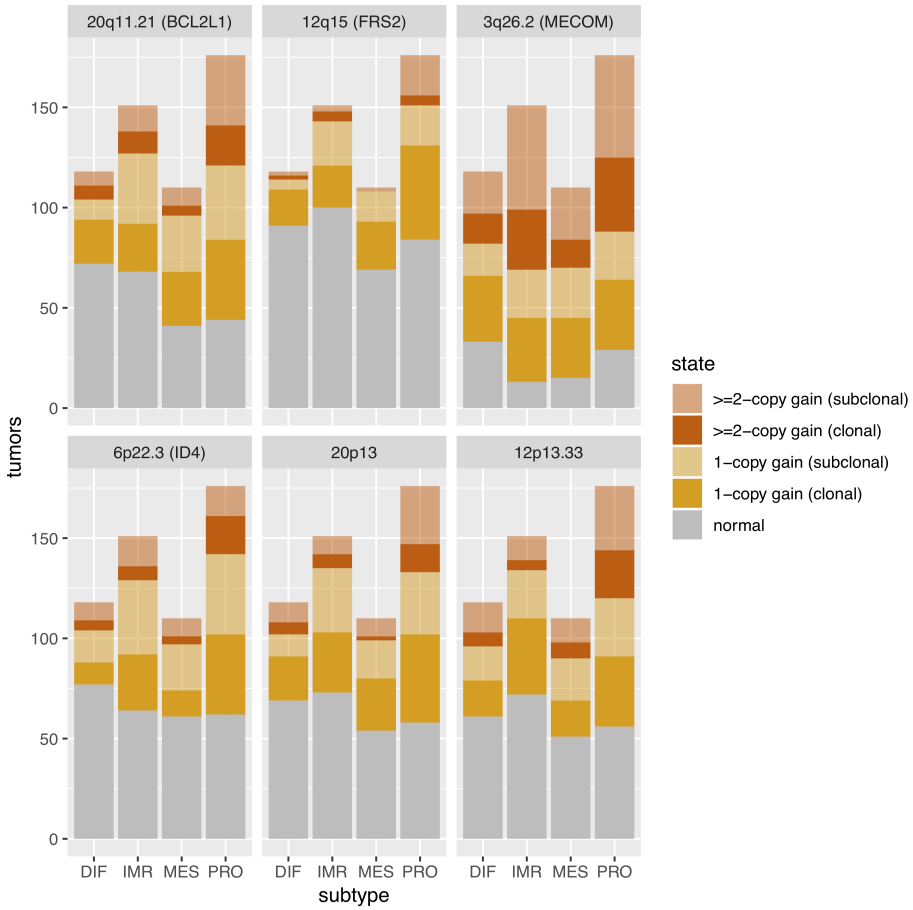

Figure S4: Top subtype-associated regions. The barplots illustrate individual `GISTIC2` regions of strongest subtype association from Figure 3C of the main manuscript. Each individual barplot displays the number of tumors (y-axis) of particular subtype (x-axis) that carry either a 1-copy gain (yellow) or $\geq$2-copy gain (red) in the region indicated at the top of each plot.

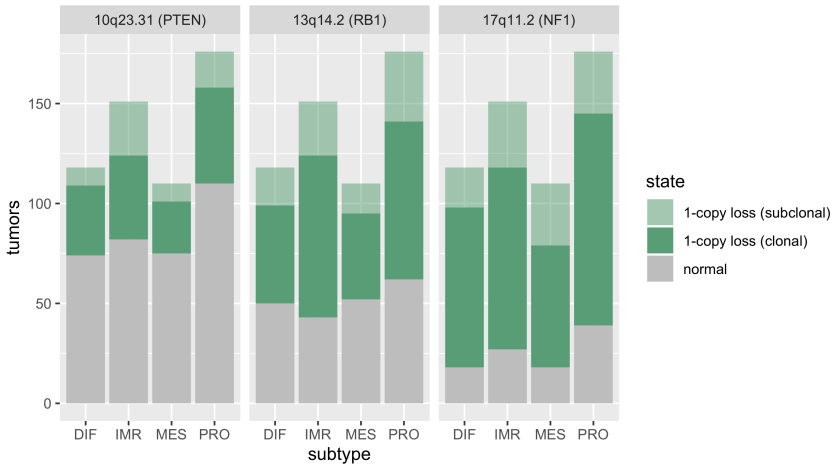

Figure S5: Regions of frequent loss. The barplots illustrate previously reported regions of frequent loss. As in Figure S4, each individual barplot displays the number of tumors (y-axis) of particular subtype (x-axis) that carry a 1-copy loss (green) either clonal (solid color) or subclonal (transparent color).

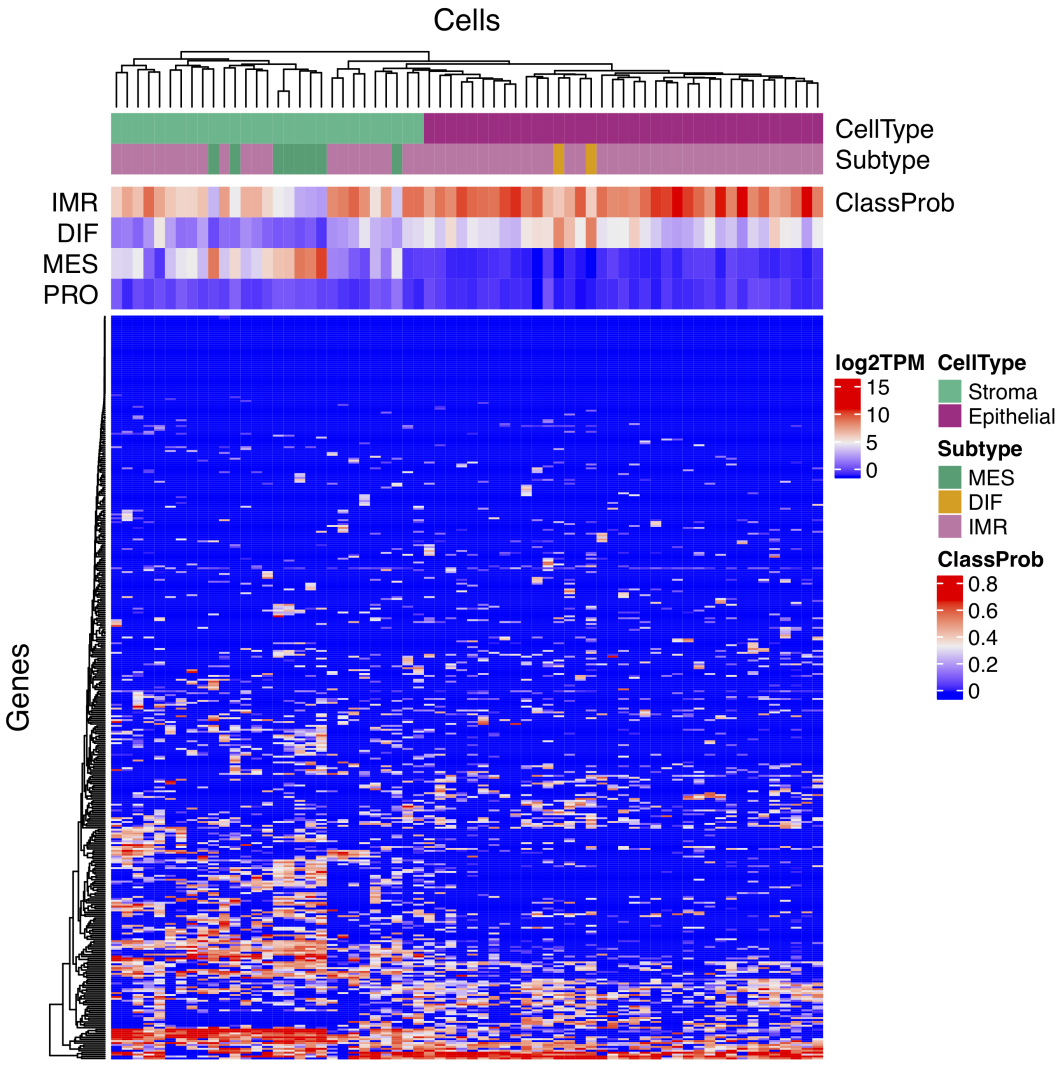

Figure S6: Single cell subtyping with 800 genes. The heatmap depicts log2 TPM expression values of the extended 800-gene signature (rows) across 66 cells (columns). The annotation bars at the top show resulting subtype calls (*Subtype*), previous characterization of cells as epithelial or stromal (*CellType*), and classification probabilities for each subtype (*ClassProb*).